Radially truncated galactic discs

Grijs, R. de; Kregel, M.; Wesson, K H

Published in:
Default journal

DOI:
10.1046/j.1365-8711.2001.04380.x

Publication date:
2000

2000

Mon. Not. R. Astron. Soc. **000**, 000–000 (2000)

Radially truncated galactic discs⋆

Richard de Grijs[1,†], Michiel Kregel[2] and Karen H. Wesson[1,‡]
[1] *Astronomy Department, University of Virginia, PO Box 3818, Charlottesville, VA 22903, USA*
[2] *Kapteyn Astronomical Institute, University of Groningen, PO Box 800, 9700 AV Groningen, the Netherlands*

Received date; accepted date

ABSTRACT
We present the first results of a systematic analysis of radially truncated exponential discs for four galaxies of a sample of disc-dominated edge-on spiral galaxies. Edge-on galaxies are very useful for the study of truncated galactic discs, since we can follow their light distributions out to larger radii than in less highly inclined galaxies. The origin of these truncations and their asymmetry and sharpness are helpful to better constrain theories of galaxy formation.
In general, the discs of our sample galaxies are truncated at similar radii on either side of their centres. With the exception of the disc of ESO 416-G25, it appears that our sample galaxies are closely symmetric, in terms of both the sharpness of their disc truncations and the truncation length. However, the truncations occur over a larger region and not as abruptly as found by van der Kruit & Searle (KS1–4).
We show that the truncated luminosity distributions of our sample galaxies, if also present in the mass distributions, comfortably meet the requirements for longevity. Stability requirements for galactic discs may play an important role in the formation and maintenance of disc truncations. A scenario in which galactic discs are truncated at the radii where the gas density becomes subcritical for star formation to occur, combined with slowly growing discs, is possibly what we observe in our sample galaxies. This hypothesis is supported by the radial $(B-I)$ colour profiles, showing that, on average, the disc colour tends to get bluer in the truncation region compared to the colours in the exponential disc.

Key words: galaxies: formation – galaxies: fundamental parameters – galaxies: photometry – galaxies: spiral – galaxies: structure

1 INTRODUCTION

It is well-known from Freeman's (1970) work that the radial light distribution of the stellar component of high surface brightness galactic discs can be approximated by an exponential law of the form

$$L(R) = L_0 \exp(-R/h_R) \quad (1)$$

where L_0 is the luminosity density in the galactic centre, R the galactocentric distance and h_R the radial disc scalelength. However, it has been shown by, e.g., van der Kruit & Searle (1981a,b, 1982a,b, hereinafter KS1–4), that at some radius $R_{\rm max}$ the stellar luminosity distribution is truncated. This radius $R_{\rm max}$, where the radial disc profile disappears asymptotically into the background noise, is often called the truncation or cut-off radius of the galactic disc. In fact, the truncation of galactic discs does not occur instantly but over a small region, where the luminosity decrease becomes much steeper, having exponential scalelengths of order or less than a kiloparsec, opposed to several kpc in the exponential disc part (e.g., KS1–4, Jensen & Thuan 1982, Sasaki 1987, Abe et al. 1999, Fry et al. 1999).

In this paper we present the first results of a systematic analysis of radially truncated exponential discs for a pilot sample of four "normal" spiral galaxies with particularly noticeable cut-offs, drawn from the statistically complete sample of edge-on disc-dominated galaxies of de Grijs (1998; see Sect. 2). The origin of these truncations and their asymmetry and sharpness are helpful to better constrain theories of galaxy formation (Sect. 4.2). If the truncations seen in the stellar light are also present in the mass distribution, they would have important dynamical consequences at the disc's outer edges (Sect. 4.3), e.g., regarding the generation and

⋆ Based on observations obtained at the European Southern Observatory, La Silla, Chile

† E-mail: grijs@virginia.edu
‡ Present address: Center for Hydrologic Science, Duke University, 106 Old Chemistry, Box 90230, Durham, NC 27708, USA

maintenance of the stellar velocity dispersion ellipsoid (e.g., KS1, van der Kruit & de Grijs 1999) and of galactic warps.

1.1 Observational status

Edge-on galaxies are very useful for the study of truncated galactic discs: since these disc cut-offs usually occur at very low surface brightness levels, they show up more readily in highly inclined galaxies, where we can follow the light distributions out to larger radii. In fact, the first detections of such cut-offs were done in a sample of 7 edge-on galaxies (KS1–4) and subsequently confirmed for some of these (e.g., Sasaki 1987 and Morrison, Boroson & Harding 1994, for NGC 5907; Lequeux, Dantel-Fort & Fort 1995, for NGC 7814; Jensen & Thuan 1982 and Näslund & Jörsäter 1997, for NGC 4565; Fry et al. 1999, for NGC 4244). For this small sample of prominent, high surface brightness edge-on spiral galaxies, the mean truncation radius $R_{\rm max} \simeq (4.2 \pm 0.6) h_R$ (KS3). The only additional galaxy for which the truncation radius was determined using the same definition, NGC 4013, has a truncated disc within this range, with the disc cut-off occurring at $\simeq 4.1 h_R$ (Bottema 1995).

Barteldrees & Dettmar (1994) found, for a sample of 27 edge-on galaxies, a mean truncation radius of $\simeq (3.7 \pm 1.0) h_R$. However, this result is based on a different definition of $R_{\rm max}$: they interpreted the truncation radius as the galactocentric distance at which the observed projected radial profiles start to deviate significantly from the model exponential profiles. If we keep in mind that the truncation occurs over a finite region, then the discrepancy between these determinations can be understood. A direct comparison is therefore impossible.

Although it is hard to detect truncations in less highly inclined galaxies, with the currently available instrumentation one should be able to detect these cut-offs, which presumably occur at a face-on surface brightness of about 26 to 27 B-mag arcsec^{-2} (KS3, van der Kruit 1988). However, the truncations are generally not seen in azimuthally averaged light profiles of less highly inclined systems (cf. Duval & Athanassoula 1983, Romanishin, Strom & Strom 1983, van der Kruit 1988, Barton & Thompson 1997, among others), due to global asymmetries in the young-disc population, such as spiral arms. Moreover, the cut-offs do not necessarily occur at the same galactocentric distances or with the same abruptness (e.g., KS1, Jensen & Thuan 1982, Näslund & Jörsäter 1997, Abe et al. 1999, Fry et al. 1999).

An interesting attempt to improve the statistics of the occurrence of radially truncated galactic discs was made by Bosma & Freeman (1993), who compared the increase of diameters (taken at the faintest perceptible isophote, where the sky background starts to dominate) of a large number of disc galaxies on various sky surveys of different photometric depths. They concluded that $\sim 26\%$ of the galaxies show only a very modest increase in diameters on the SRC-J survey compared to the shallower Palomar sky survey plates, indicating the presence of a cut-off in the outer disc. For galaxies with an exponential disc with central surface brightness $\mu_0 = 21.65$ B-mag arcsec^{-2} (Freeman 1970), they find that the disc has to truncate at a radius of less than $\sim 3.5 h_R$, which is at significantly smaller radii than found by KS1–4 and van der Kruit (1988), but of the same order as the mean cut-off radius of Romanishin et al. (1983; $R_{\rm max}/h_R \simeq 2.8 \pm 0.6$) for their sample of spirals with *low surface brightness* discs.

However, most of these comparison samples contain galaxies seen under various angles with respect to the line of sight, and therefore one has to be cautious in interpreting these results. Barteldrees & Dettmar (1994) warn that inclination effects are important when dealing with edge-on galaxies: if one neglects a deviation from an exactly 90° inclined orientation, one will underestimate the truncation radius compared to the edge-on orientation. Thus, an independent approach to obtain the statistics of truncated galactic discs, using a sample of galaxies selected in a uniform way, is needed in order to better understand the overall properties and physical implications of this feature. In this paper we present the first results of such a study.

1.2 The Galaxy

Due to our position within the Galactic disc, the determination of a cut-off in the Galactic stellar disc luminosity and/or mass distribution is a complicated issue. KS3 and Lacey & Fall (1985) were among the first to argue that the Galactic disc is likely truncated, based on the observations of Chromey (1978) of the distribution of OB stars in the anticentre direction, which indicates a sharp decline beyond $R_{\rm max} \approx 20$ kpc. In addition, Fich & Blitz (1984) and Fich et al. (1989) found that the distribution of HII regions ends beyond $R_{\rm max} \approx 16 - 20$ kpc, while strong warping of the HI layer begins at $R \approx 13 - 17$ kpc (Henderson et al. 1982, Kulkarni, Blitz & Heiles 1982, Burton 1988, Porcel, Battaner & Jiménez-Vicente 1997). This is often thought to coincide with an end to the stellar mass distribution (Sancisi 1983, Bottema 1995). As pointed out by Robin, Crézé & Mohan (1992b), Wouterloot et al. (1990) detected a sharp decline of the CO density at $R \sim 18 - 20$ kpc, indicating that star formation ceases at approximately this radius.

More recently, Freudenreich et al. (1994), Porcel et al. (1997), and Freudenreich (1998) concluded, based on observations with the *DIRBE* experiment on board *COBE*, that the apparent displacement between the Galactic warp traced by the stellar and the HI discs is most likely the signature of a stellar disc with a cut-off at $R_{\rm max} \leq 15$ kpc. This is consistent with recent results obtained by the *DENIS* team (Ruphy et al. 1996; they favour a disc truncation at $R_{\rm max} = (15 \pm 2)$ kpc) and by Robin et al. (1992a,b), who obtained a similar result based on deep optical star counts towards the Galactic anticentre.

In spite of these studies, the radius at which the Galactic disc truncates is still an open issue; it depends on the adopted disc scalelength and the population studied to trace the disc mass (e.g., Robin et al. 1992a). Based on the recent determinations of the Galactic disc scalelength in the anticentre direction of (2.5 ± 0.3) kpc (Robin et al. 1992a,b) and a solar Galactocentric distance of $R_\odot = 8.5$ kpc, $R_{\rm max} = (5.6 \pm 0.6) h_R$ (see also Freudenreich 1998), which is consistent with the determinations of truncation radii in other galaxies by KS1–4.

2 APPROACH

We will approximate the three-dimensional luminosity density of the discs of edge-on spiral galaxies as a combination of independent exponential light distributions in both the radial and the vertical directions (see, e.g., de Grijs, Peletier & van der Kruit [1997] for a statistical approach to determine the latter behaviour), for all radii excluding the region of truncation. In view of the finite extent of the cut-off region, δ, and to avoid discontinuities in the luminosity and density distributions, we will adopt Casertano's (1983) mathematically convenient description for a "soft cut-off" of the radial density distribution in the truncation region. This assumes that in the region beyond $(R_{\rm max} - \delta)$, the radial luminosity density decreases linearly to zero:

$$L(R) = L_0 \begin{cases} \exp(-R/h_R), & \\ & \text{if } R \leq (R_{\rm max} - \delta) \\ \exp\big(-(R_{\rm max} - \delta)/h_R\big) \Big[1 - \Big(R - (R_{\rm max} - \delta)\Big)\Big], & \\ & \text{if } (R_{\rm max} - \delta) \leq R \leq R_{\rm max} \\ 0, & \text{if } R > R_{\rm max}. \end{cases} \quad (2)$$

The exact functional form of the radial luminosity density in the cut-off region is unknown because of the limited spatial resolution and low signal-to-noise (S/N) ratio at these large galactocentric distances. Thus, within the observational uncertainties, Casertano's (1983) description of the "soft cut-off" does not deviate significantly from the simple exponential form adopted by Jensen & Thuan (1982) and Näslund & Jörsäter (1997) to fit the truncated light profiles of NGC 4565. In addition, fitting our galaxies' radial luminosity profiles to Eq. (2) also allows us to determine the (projected) physical extent of the truncation region.

The total three-dimensional luminosity density is now given by

$$L(R, z) = L(R) \exp(-z/h_z) \quad , \quad (3)$$

where z is the (vertical) distance from the galactic plane and h_z the exponential scaleheight. We will use this approximation for the simultaneous determination of the radial and vertical scale parameters (Sect. 2.3).

2.1 Pilot sample

As we argued in Sect. 1.1, sharply truncated galactic discs are best studied in edge-on galaxies, where we can trace the light distribution further out due to projection along the line of sight. We selected four galaxies from the statistically complete sample of disc-dominated edge-on galaxies of de Grijs (1998) for a detailed pilot study of their two-dimensional (2D) surface brightness distributions.

The galaxies in the parent sample were selected to:

- have inclinations $i \geq 87^\circ$;
- have blue angular diameters $D^B_{25} \geq 2.'2$; and
- be non-interacting and undisturbed S0 – Sd galaxies.

The basic physical properties of the galaxies in our pilot sample are summarised in Table 1 (data are taken from de Grijs 1998 unless otherwise indicated); the detailed observational logs and data reduction techniques of our *B, V* and *I*-band observations are summarised in de Grijs (1998). Fig. 1 displays the *I*-band contours of these galaxies. Note that an indication of the presence of disc truncations is already given by the rounded contours at the discs' outer edges.

2.2 Scalelength determinations

2.2.1 Deviations from exponential light distributions

A number of previous studies have suggested that the cut-offs in "normal" disc galaxies generally occur at similar radii, expressed in units of the disc scalelength (Sect. 1.1). If we want to test this hypothesis, we obviously need good estimates of the exponential scale parameters of the galactic discs in our sample. However, Knapen & van der Kruit (1991), among others, have shown that the scalelengths of a particular galaxy, determined by different authors, may vary by as much as 20%. The scalelength determinations depend heavily on the radial fitting range, because in general the radial profiles are not exactly exponential (e.g., Seiden, Schulman & Elmegreen 1984, Shaw & Gilmore 1990, de Jong 1995, and references therein).

In the case of an edge-on orientation, our model radial exponential luminosity density distribution projects onto the plane of the sky as (KS1):

$$L(R) = L_0 \frac{R}{h_R} K_1\Big(\frac{R}{h_R}\Big), \quad (4)$$

where K_1 is the modified Bessel function of the first order.

Even though Eq. (4) simplifies at large radii ($R/h_R \gg 1$) to (KS1):

$$L(R) = L_0 \Big(\frac{\pi R}{2h_R}\Big)^{1/2} \exp(-R/h_R), \quad (5)$$

implying that the functional form of Eq. (4) at large radii is similar to the intrinsic exponential profile, the value of the measured scalelength depends critically on the choice of the inner fitting boundary, since the projected profiles deviate significantly from exponential light distributions at smaller radii.

In Fig. 2a we show both the radial surface brightness distribution corresponding to the exponential luminosity density of Eq. (1), and the effects of projection and line-of-sight integration in the case of edge-on galaxies, Eq. (4). From this panel it can already be appreciated that one should be cautious in choosing the boundaries of the radial range to determine exponential scalelengths. Fig. 2b shows the effects of varying the inner fitting boundary, $R_{\rm min}$, with respect to the maximum fitting boundary, which was taken at $4h_R$. From this figure, it follows that projection and line-of-sight integration effects have caused de Grijs (1998) to overestimate the radial disc scalelengths by up to $\sim 20\%$, by assuming an intrinsic exponential light distribution. The maximum fitting radius at $4h_R$ was chosen to ensure a sufficiently high S/N ratio and by the necessity to include as much emission of the outer discs as possible (de Grijs 1998).

Secondly, a patchy dust distribution in a particular galaxy can easily lead to varying estimates of the scalelength, depending on the way the data is reduced and analysed (e.g., Giovanelli et al. 1994).

Finally, the signature of a gradual thickening of a galactic disc is to flatten its (projected) radial surface brightness profile and hence artificially increase the measured scalelength (Sect. 2.2.2).

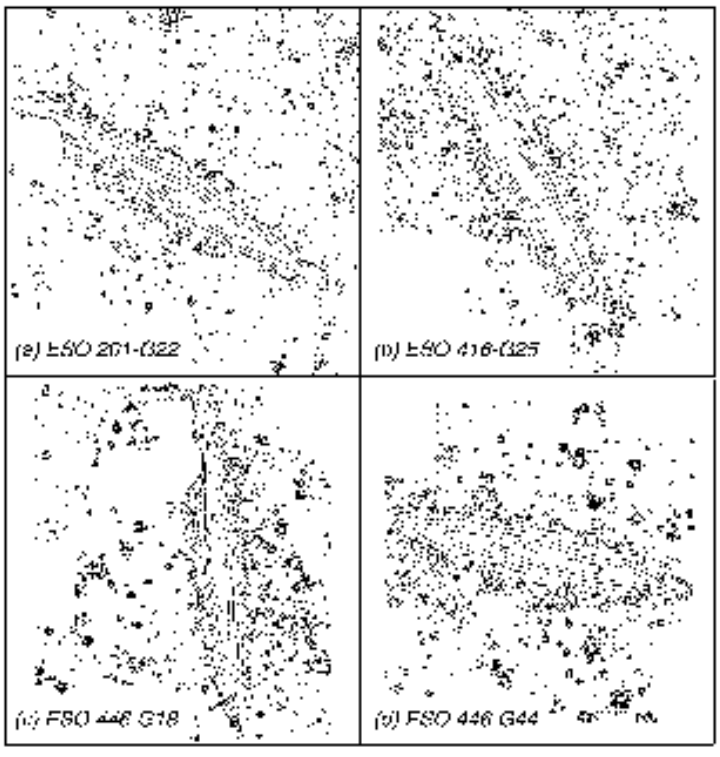
(a) ESO 201-G22
(b) ESO 416-G25
(c) FSO 446 G18
(d) FSO 446 G44

Table 1. Basic properties of the pilot sample galaxies
Columns: (1) Galaxy name (Lauberts & Valentijn 1989; ESO-LV); (2) and (3) Coordinates; (4) Revised Hubble Type; (5) Blue major axis diameter, D_{25}^B (de Grijs 1997 [Chapter 2]); (6) Passband observed in; (7) and (8) apparent magnitude and observational error, corrected for foreground extinction; (9) and (10) extrapolated edge-on disc central surface brightness and uncertainty; (11) and (12) Exponential scaleheight ($\pm 0.''03$); (12)–(15) Exponential scalelength and observational error.

Galaxy	RA (J2000)	Dec	Type	D_{25}^B	Passband	m_0	$\pm$	μ_0	$\pm$	h_z		h_R	$\pm$	h_R	$\pm$
	($^{\rm h}$ $^{\rm m}$ $^{\rm s}$)	($^\circ$ $'$ $''$)	(T)	($'$)		(mag)		(mag arcsec^{-2})		($''$)	(h^{-1} kpc)	($''$)		(h^{-1} kpc)	
(1)	(2)	(3)	(4)	(5)	(6)	(7)	(8)	(9)	(10)	(11)	(12)	(13)	(14)	(14)	(15)
ESO 201-G22	04 08 59.3	−48 43 42	5.0	2.52	*B*	14.06	0.07	19.36	0.67			31.08	0.81	6.67	0.17
					I	13.10	0.03	18.28	0.11	3.01	0.65	21.98	0.42	4.72	0.09
ESO 416-G25	02 48 40.8	−31 32 07	3.0	2.35	*B*	14.42	0.11	20.65	0.09			12.94	0.66	3.59	0.18
					I	12.52	0.03	18.44	0.08	3.47	0.96	11.28	0.49	3.13	0.13
ESO 446-G18	14 08 37.9	−29 34 20	3.0	2.52	*B*	15.12	0.05	20.96	0.09			22.38	0.64	5.38	0.15
					I	12.71	0.02	18.74	0.05	2.27	0.55	16.60	0.36	3.99	0.09
ESO 446-G44	14 17 49.3	−31 20 55	6.0	2.67	*B*	14.83	0.03	22.49	0.20			52.00	5.05	8.17	0.79
(= IC 4393)					*I*	12.51	0.04	19.82	0.09	2.56	0.40	27.88	1.08	4.38	0.17

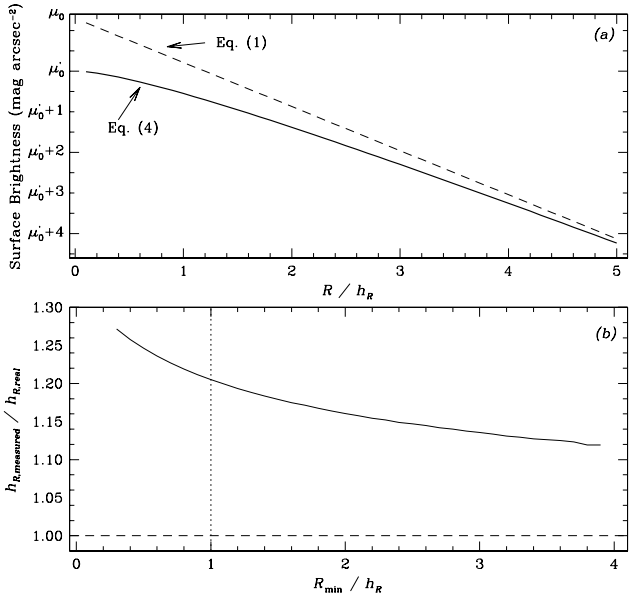

Figure 2. *(a)* – Radial surface brightness profile seen in face-on disc galaxies (dashed line; Eq. (1)) and projected, edge-on profile resulting from line-of-sight integration, assuming the same scalelength and face-on central surface brightness μ_0 (solid line; Eq. (4)). μ_0' is the projected edge-on central surface brightness. *(b)* – Ratio of the actual measured scalelengths to the model radial scale parameter, determined between the minimum fitting boundary $R_{\rm min}$ and the maximum fitting boundary at $4h_R$ (de Grijs 1998). The vertical dotted line indicates $R_{\rm min} = 1h_R$ used by de Grijs (1998), and shows that his scalelengths are too large by up to $\sim 20\%$.

These effects may, in fact, contribute significantly to the scatter in the mean values of the cut-off radii quoted by KS1–4, van der Kruit (1988), and Barteldrees & Dettmar (1994).

2.2.2 Luminosity profiles parallel to the major axis

The simplest approach to study the occurrence of disc cut-offs is by analysing radial luminosity profiles, extracted along or parallel to a galaxy's major axis. Since we are dealing with edge-on galaxies, the inner disc region closest to the plane often needs to be avoided because of the presence of either a prominent dust lane, or a patchy dust distribution with its highest density towards the galactic plane (cf., e.g., de Grijs et al. 1997). In many cases, the dust component extends all the way to the edge of the disc, thus making the luminosity profiles in the galactic planes useless for our purpose, in particular in optical passbands.

The exponential scale*height* of galactic discs is – to first order – constant as a function of (projected) galactocentric distance, at least for later-type disc galaxies (see, e.g., KS1–4, Kylafis & Bahcall 1987, Shaw & Gilmore 1990, Barnaby & Thronson 1992, de Grijs & Peletier 1997). Therefore, the radial luminosity distributions parallel to the galactic planes show a similar functional behaviour as the luminosity profiles *in* the plane in the absence of the dust component. Consequently, by extracting light profiles parallel to the galactic planes, we will also be able to study the occurrence of radially truncated discs, provided that the S/N ratio allows us to detect such a truncation.

To find the optimum balance between avoiding contamination by the in-plane dust component on the one hand, and retaining a sufficiently high S/N ratio at large galactocentric distances on the other, numerous experiments were performed.

In Fig. 3 we show ESO 416-G25 as an example, where we compare several radial profiles obtained on either side of the galactic plane. The solid lines in both panels represent the total profiles, vertically averaged over the entire half of the galactic disc (effectively for $|z| \leq 8h_z$). They are obviously significantly affected by either patchy dust and low S/N re-

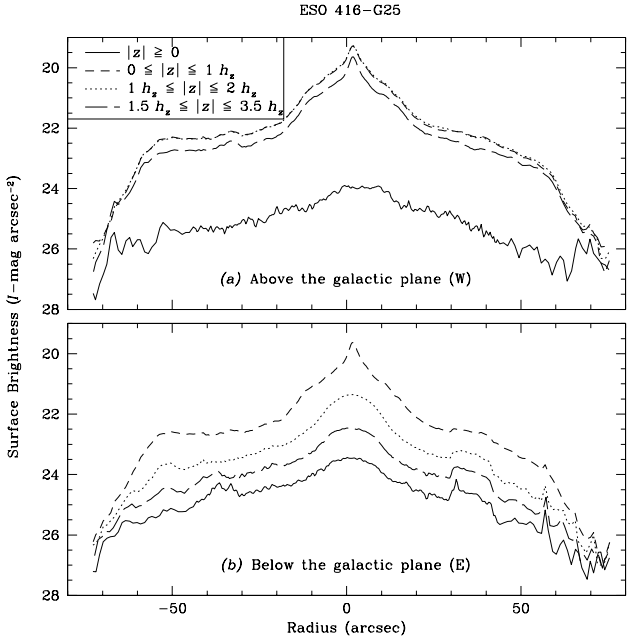

Figure 3. Vertically averaged radial surface brightness profiles of ESO 416-G25, taken at various z-heights from the galactic plane. To retain an approximately constant S/N ratio, a semi-logarithmic intensity-weighted radial binning algorithm has been applied to the individual profiles. An indication of the observational uncertainites is given by the noise features in the individual profiles.

gions throughout the disc and are therefore discarded from further use. Even though this galaxy does not have a prominent dust lane nor a very large amount of patchy extinction throughout its disc, Fig. 3 clearly shows the rationale behind choosing the least obscured side of the galactic disc (top panel). Keeping in mind our purpose of determining the presence of a sharp cut-off at the disc's outer edge, it follows from a close examination of this figure (and similar figures for the other galaxies in our sample) that either the range $(1.0 \leq |z| \leq 2.0 h_z)$ or $(1.5 \leq |z| \leq 3.5 h_z)$ is preferred for our detailed analysis. Since the former region has in general a higher S/N ratio we conclude that the most representative, unobscured light profiles are obtained by vertically collapsing the surface brightness distribution between 1 and 2 h_z *on the least obscured side of the galactic plane.*

In the radial direction, we apply a semi-logarithmic binning algorithm, in order to retain an approximately constant overall S/N ratio, where the binning at the outermost disc radii never exceeds 2 resolution elements needed to resolve the truncation region (cf. de Grijs et al. 1997, de Grijs 1998).

A potential problem of this method is that the S/N ratios in the outer disc regions are often significantly lower at some (vertical) distance from the galactic planes compared to those in the planes. This may affect the resulting values for radial truncations in the light distributions. Close examination of Fig. 3 (and similar figures for the other sample galaxies) shows, however, that although the radial extent of the cut-off region (δ; cf. Eq. (2)) appears to be only a weak function of the height from the planes, the actual radii at which the luminosity profiles disappear asymptotically into the background noise converge to the same value of $R_{\rm max}$, within the observational uncertainties.

In addition, some evidence exists that galactic discs thicken (i.e., have greater scaleheights) with increasing galactocentric distance (e.g., KS1, Kent, Dame & Fazio 1991, Barnaby & Thronson 1992, de Grijs & van der Kruit 1996, de Grijs & Peletier 1997). The signature of such a thickening of the discs on light profiles extracted parallel to the galaxies' major axes would be either a flattening of the radial surface brightness profiles (if the thickening occurs gradually; e.g., Kent et al. 1991, Barnaby & Thronson 1992, de Grijs & Peletier 1997) or a locally enhanced surface brightness level at these large galactocentric distances (if only the outermost profiles are affected; e.g., KS1, de Grijs & van der Kruit 1996). However, de Grijs & Peletier (1997) have shown that the effects of disc thickening are largest for the earliest-type spiral galaxies and almost zero for the later types, including those examined in detail in this paper. Moreover, even though the discs of our sample galaxies may have larger scaleheights with increasing radii, the low S/N ratios and deviations from exponentially decreasing luminosity distributions due to, e.g., spiral arms will likely hide such observational signatures. Finally, the possible thickening of galactic discs will probably *not* affect the determination of the actual truncation *radius* $R_{\rm max}$, since the *radial* luminosity distribution remains likely unaffected. If the thickening only occurs in the truncation region, it may artificially steepen the radial scale parameter *in this region*, although the *extent* of the truncation area will likely not be affected.

To determine the properties of the disc truncations in our sample galaxies, we will assume that the functional form of Eq. (2) closely approximates the radial surface brightness profiles. Although line-of-sight projection affects the observed functional form of the radial luminosity distribution, we will use an unmodified version of Eq. (2) to model the truncations in our sample galaxies. We chose to do so, because (i) Eq. (2) is a mathematically convenient functionality (without any strong physical motivation), and (ii) the actual profile shapes in the truncation region are erratic due to low S/N ratios and therefore the assumption of any more complicated functionality than a linearly decreasing luminosity density cannot be taken seriously.

Finally, we will compare the cut-off radii found using this method with quantitative comparison of the observed 2D image to a model image of a projected exponential disc, in both the radial and vertical directions, both with and without a sharply truncated disc. This will give us an independent confirmation of the cut-offs (e.g., van der Kruit 1989).

2.3 Two-dimensional surface brightness modelling

The surface brightness distributions of spiral galaxies often show significant local deviations from the assumed smooth, large-scale model distributions (e.g., Shaw & Gilmore 1990, de Jong 1995). This makes the global applicability of radial disc scalelengths obtained from single radial profiles of edge-on galaxies very uncertain (e.g., Sect. 2.2.1).

Therefore, here we will first obtain accurate estimates

of the radial scalelengths based on 2D surface brightness fitting of the galactic discs in our sample, using Eqs. (3) and (4), and then use these to study deviations of the galaxies' radial profiles from exponential discs and the occurrence of radial disc truncations in the remainder of this paper. In this section we give a description of the method, the results will be presented in Sect. 3.4. A more elaborate description of the method, as well as extensive tests on artificial images, will be presented in Kregel, van der Kruit & de Grijs (in preparation).

A number of potential problems are foreseen regarding the applicability of our simple 2D model to the observed luminosity distributions of edge-on galaxies. First, it does not include a description for the truncation region. A physically motivated, or even an empirical 2D description of this region is, at this point, too premature and therefore this region will be masked out before least-squares minimization. Secondly, the regions near the galactic planes are affected by extinction effects. Whilst this effect can be included by using a three-dimensional radiative transfer code (e.g., Kylafis & Bahcall 1987, Xilouris et al. 1997), we choose to mask the data in the regions near the planes instead for the determination of the radial scalelengths (see Sect. 3.1 for a description of this method for the individual sample galaxies).

Finally, the presence of an additional central component, such as a bulge or bar, further complicates the analysis. Examination of Fig. 1 shows that three of our sample galaxies show such a component. In these cases, we introduce an additional component, parametrized by an exponential bulge model (Andredakis & Sanders 1994),

$$\mu_{\rm bulge}(R,z) = 5.360\mu_e\ e^{-1.679\sqrt{R^2+(z/q)^2}/r_e}, \qquad (6)$$

where r_e is the effective radius, μ_e the effective surface brightness and q the axis ratio of the central component. To account for the effects of seeing the model bulge is convolved with a Gaussian PSF (for the disc component the effects of seeing are negligible; de Jong 1995, Kregel et al., in prep.). In Sect. 3.1 we will compare the results of fitting this disc+bulge model and those of the disc-only model. Since the central region of the bulge will be masked out automatically by the dust mask, a fit to the more compact bulges can turn out to be underconstrained (Kregel et al., in prep.).

The fitting algorithm employs the non-linear least-squares technique developed by Marquardt (1963). The fits were performed on the sky-subtracted images. To minimize the relative errors between observed and model values, each unmasked pixel was given a weight inversely proportional to the model surface brightness distribution constructed from the initial estimates (de Jong 1995).

However, before applying our 2D surface brightness modelling routine, the sky-subtracted images needed to be prepared. First, foreground stars and background galaxies were masked out. Secondly, profiles parallel to the minor axis were taken at various distances along the major axis. These were subsequently inspected for extinction effects, leading to the masking out of the regions described in Sect. 3.1.

Table 2. Global scale parameters obtained from the 2D fitting method

Columns: (1) Galaxy name; (2) Passband observed in; (3)–(4) Edge-on disc central surface brightness, assuming an exponential disc in both the radial and vertical directions, and observational error; (5)–(6) Exponential scalelength and observational error.

Galaxy	Passband	μ_0	$\pm$	h_z	$\pm$	h_R	$\pm$
		(mag arcsec^{-2})		($''$)		($''$)	
(1)	(2)	(3)	(4)	(5)	(6)	(7)	(8)
ESO 201-G22	*B*	20.54	0.07	2.4	0.1	26.9	1.5
	V	20.39	0.10	2.4	0.1	25.2	1.1
	I	19.23	0.08	2.6	0.2	23.3	1.3
ESO 416-G25	*B*	21.41	0.03	3.1	0.1	29.2	1.4
	V	20.90	0.08	3.5	0.2	25.8	1.3
	I	19.87	0.05	3.6	0.2	22.2	2.0
ESO 446-G18	*B*	20.72	0.10	2.2	0.1	22.5	1.3
	V	20.03	0.08	2.2	0.1	19.5	0.9
	I	18.49	0.10	2.0	0.2	18.1	1.4
ESO 446-G44	*B*	20.39	0.10	2.1	0.1	25.1	0.7
	V	19.76	0.07	2.0	0.1	24.5	0.6
	I	18.90	0.15	2.7	0.2	29.5	1.6

3 RESULTS AND ANALYSIS

3.1 Two-dimensional scalelength determination

In Table 2 we present the global scale parameters of our pilot sample galaxies, obtained from the 2D fitting method described in Sect. 2.3. The uncertainties in the scale parameters listed in this table are the observational errors, estimated by comparing results from several similar fits in which we adjusted the boundaries of the radial fitting range by 10–20%; the formal errors were in general less than 1%.

In the following, we will discuss the fits to the luminosity density of each galaxy individually, thereby highlighting a number of problems encountered in each case. In all fits the galactic centres were fixed at the values determined by fitting ellipses to the *I*-band images. Fig. 4 shows the *I*-band images and residual emission (disc model subtracted from the observed luminosity distribution) for ESO 201-G22 and ESO 416-G25.

In each case, conservative estimates of the onset of the truncation region and of the region near the galactic plane most heavily affected by extinction were made based on detailed visual examinations of the radial and vertical luminosity distributions, respectively. The inner boundaries used for the radial fitting were chosen to minimize possible bulge effects and will be discussed individually below. Table 3 summarizes the radial ranges adopted for the disc fits, as well as the vertical ranges excluded to avoid extinction effects.

ESO 201-G22 – Figs. 4a and b clearly show the bulge component and, just outside the masked region, the effects of either residual extinction near the galactic plane or, more likely, an additional disc component. The residuals in the fitted region do not show large systematic effects, and therefore the effect of any bulge contribution within this region is likely small. We checked this by fitting a disc+bulge model to the *I*-band data. This fit resulted in similar disc parameters as obtained

Table 3. 2D fitting regions
Columns: (1) Galaxy name; (2) and (3) Radial fitting range (arcsec); (4) and (5) Vertical region around the galactic plane excluded from the 2D fits (h_z).

Galaxy	Radial fitting		Galactic plane	
	$r_{\rm min}$	$r_{\rm max}$	$z_{\rm min}$	$z_{\rm max}$
(1)	(2)	(3)	(4)	(5)
ESO 201-G22	15	50	–1.0 (S)	1.0 (N)
ESO 416-G25	25	50	–1.0 (E)	1.0 (W)
ESO 446-G18	18	55	–2.0 (E)	0.5 (W)
ESO 446-G44	0	36	–1.5 (S)	1.5 (N)

from the disc-only fit; the best-fitting bulge parameters are $\mu_e = 21.2$ I-mag arcsec^{-2}, $r_e = 9.''9$, and $q = 0.52$. Thus, the bulge contribution to the disc-dominated fitting range is negligible. The negative residuals extending to the edges of these figures clearly show the presence of a truncation in the galactic light distribution.

ESO 416-G25 – This is the earliest-type galaxy in our pilot sample, and also contains the most prominent bulge. The residuals after subtracting the disc-only fit (Fig. 4d) do not appear to be systematic in the region where the fit was done, and their amplitude is small (r.m.s. residual $\approx 1.7\ \sigma_{\rm background}$). Minor-axis profiles (Fig. 3) show that the bulge does not extend much further out of the plane than the disc. Although we included an exponential bulge component, the 6-parameter fit proved to be very unstable. Due to the unknown, but likely small, bulge contribution in the region in which the 2D fitting routine was applied, our scalelength estimate is a firm lower limit.

ESO 446-G18 – Fig. 1c shows that this galaxy is not exactly edge-on. This is even more obvious in the minor-axis profile of Fig. 5. Extinction predominantly affects the eastern side. A dust mask placed symmetrically with respect to the major axis, as applied for ESO 201-G22 and ESO 416-G25, is therefore not appropriate. The residuals are large (r.m.s. residual $\approx 3.3\ \sigma_{\rm background}$) but do not appear to be systematic in the region where the fit was done. A similar fit including an exponential bulge did not converge.

ESO 446-G44 – Surface brightness profiles of ESO 446-G44 do not reveal any bulge component. They do show, however, that ESO 446-G44 may not be exactly edge-on. Again, the residuals in the region where we applied our 2D fitting routine are large (r.m.s. residual $\approx 5.3\ \sigma_{\rm background}$) but do not appear to be systematic.

3.2 Global comparison between the one- and two-dimensional approaches

When we compare the global scale parameters of our pilot sample galaxies, obtained from the 2D fitting method (Table 2), with the one-dimensional (1D) fit results obtained by de Grijs (1998; Table 1), we notice a strong disagreement between the results for ESO 416-G25. Close examination of the surface brightness distribution of this galaxy reveals that its highly non-exponential radial light profile and prominent bulge are the likely causes of the discrepancy; it also shows that the 2D results approximate the radial light distribution more closely than the de Grijs (1998) 1D results. On

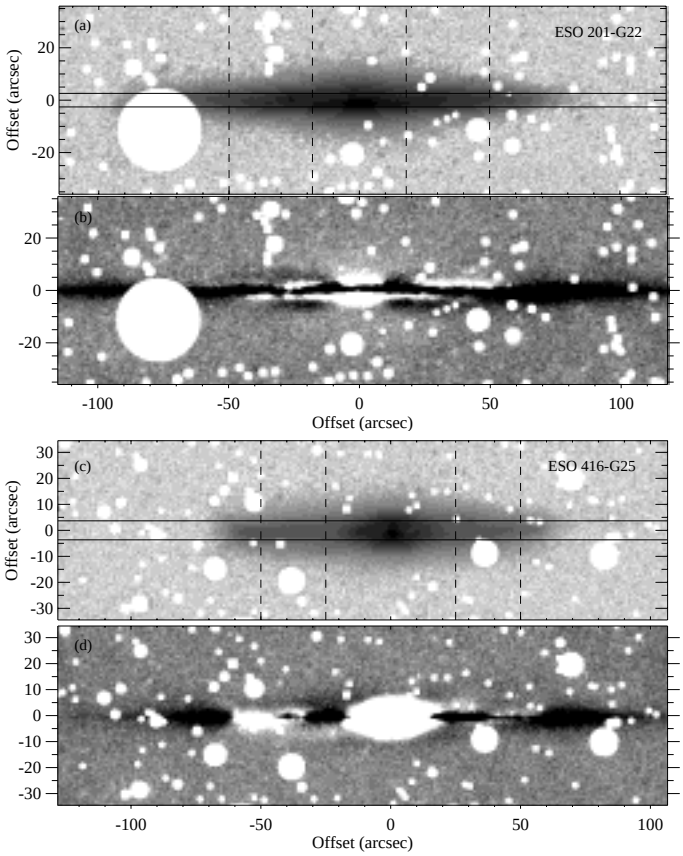

Figure 4. *(a)* – Negative I-band image of ESO 201-G22, after removal of foreground stars and background galaxies. The radial fitting boundaries are indicated by the dashed lines; the dust mask covering the region close to the plane affected by extinction is bracketed by the solid lines; *(b)* – Residuals for ESO 201-G22 after subtracting the model, greyscale levels range from $-6\sigma_{\rm background}$ (black) to $+6\sigma_{\rm background}$ (white) *(c)* and *(d)* – ESO 416-G25, as (a) and (b)

average, the resulting scaleheights from the 2D method appear to be smaller than those obtained from the 1D fits, although they are generally similar, within their uncertainties. The I-band scalelengths do not show any strong systematic differences. The B-band scalelengths are heavily affected by the extinction and will therefore be highly dependent on the assumed radial fitting range, so that a comparison between the scale parameters in this passband becomes uninteresting. For our four sample galaxies we measure differences between both methods of up to $\sim 29\%$ for the resulting values for the (I-band) exponential scaleheights and, if we exclude the discrepant results for ESO 416-G25, up to $\sim 25\%$ for the I-band radial exponential scale parameters. In Kregel et al. (in prep.) we will analyse the systematic differences between both methods for the entire de Grijs (1998) sample.

3.2.1 Scalelength comparisons

The differences in our scalelength determinations can be explained as a combination of effects due to:

(i) the choice of the radial fitting range;
(ii) the fitting model;

(iii) non-constancy of the vertical scaleheight;
(iv) residual, patchy extinction at large z heights.

The choice of the radial fitting range – The scalelengths of a particular galaxy, determined by different authors, may vary by as much as 20% (e.g., Knapen & van der Kruit 1991). The strong dependence on the adopted radial fitting range is due to deviations from radial exponential profiles seen in most spiral galaxies (Sect. 2.2.1). For the determination of his scalelengths, de Grijs (1998) used a radial range between 1 and $4h_{R,I}$, while for our 2D fitting method we used the *two-dimensional* luminosity density distribution (in individually selected areas) to constrain our fits. If we exclude the erroneous 1D result for ESO 416-G25, the differences between both methods do not appear to be systematic, however.

The fitting model – As we also showed in Sect. 2.2.1, the scalelengths determined by de Grijs (1998) are likely overestimated by up to $\sim 7\%$ because of his use of an exponential light profile, instead of an exponential radial luminosity distribution *projected along the line of sight*, Eq. (4).

Non-constancy of the vertical scaleheight – De Grijs & Peletier (1997) show that in many cases the vertical disc scaleheights appear to increase with galactocentric distance. Although we do not believe this to be a significant effect (Sect. 2.2.2), if present, it will slightly increase the measured scalelengths. This effect will be larger for the 2D fitting method, because for these fits we use a greater vertical fitting range.

Residual extinction – Since the 2D fitting method is based on the observed luminosity distribution on both sides of the galactic planes, whereas the 1D method only takes into account the surface brightness on the side least affected by dust, the 2D method will be more prone to the effects of residual, likely patchy extinction at greater z heights. Because of the way we chose to weigh the data points, this effect will be more accentuated than for the 1D method. Since the dust component is generally more concentrated towards the galactic centres, the effects of residual extinction at $z > 0$ will lead to overestimated scalelengths.

3.2.2 Scaleheight comparisons

The measured differences in the vertical scaleheights between both methods are likely due to a combination of effects such as:

(i) the vertical fitting range and the inclusion of regions affected by residual dust;
(ii) the fitting model;
(iii) the non-exponentiality of the radial luminosity profiles.

It appears that, although de Grijs et al. (1997) and de Grijs (1998) based their scaleheight determinations on near-infrared observations, if available, the choice of passband does not significantly affect the observed old-disc scaleheight, based on 1D vertical profiles (e.g., de Grijs & van der Kruit 1996, de Grijs & Peletier 1997, de Grijs 1998).

The choice of the vertical fitting range; residual dust effects – As for the fitting of the radial scalelengths, the choice of the vertical fitting range, and therefore the amount of residual dust included in the fits, will similarly affect the vertical scale parameters.

The fitting model – Since de Grijs et al. (1997) based their scaleheight estimates on the detailed modelling of their K'-band observations, we believe that the 1D scaleheights are more accurate than the 2D results.

Non-exponentiality of the radial profiles – In our 2D modelling we have assumed that our galactic discs exhibit perfect radial exponential luminosity profiles. However, as can be seen from, e.g., Figs. 5 (right-hand panels) and 6, the radial surface brightness profiles of all our sample galaxies show noticeable deviations from an exponential behaviour. Forcing our model fits to adopt a single radial exponential scalelength will therefore cause the resulting vertical scale parameter to be significantly off.

3.3 Truncated discs: Concerns

In interpreting the steep luminosity decline as truly representative of a decrease in either the light or density distributions of a galactic disc, one has to make sure that the observed cut-off is not an artifact due to inaccurate sky subtraction. De Vaucouleurs (1948), de Vaucouleurs & Capaccioli (1979), and also van Dokkum et al. (1994) have shown that inaccurate sky subtraction (i.e., oversubtraction) causes a false cut-off in the luminosity distribution of a galactic disc. This can easily be checked, because the artificial cut-off would not only be present in a major axis cut, but also in cuts taken in other directions.

In all cases, the background emission in the field of view of our sample galaxies could be well represented by a plane, of which the slope was determined by the flux in regions sufficiently far away from the galaxies themselves in order not to be affected by residual galactic light. For the majority of our observations, these planes were closely approximated by constant flux values across the CCD field. The remaining uncertainties in the background are largely due to poisson noise.

Fig. 5 illustrates the quality of the background subtraction in the I band, where the background contribution is greater than in our other optical passbands. The left-hand panels show the minor-axis surface brightness profiles of all sample galaxies (solid lines), radially averaged over $\sim 20''$, in order to be able to reach similar or fainter light levels as for the profiles along the major axes, shown in the right-hand panels. We determined the sky noise, σ, in the regions used for the background subtraction and created new images by subtracting (background -2σ), (background -1σ), (background $+1\sigma$), and (background $+2\sigma$), where "background" represents our best estimate of the sky background in the individual images (Fig. 5).

The effects of oversubtraction can clearly be seen in the minor-axis surface brightness profiles: they show artificial cut-offs and the negative background values result in undefined surface brightnesses at these z heights, above or below $\approx 15''$. Although the effects of oversubtraction on the major-axis profiles show similar false cut-offs as for the minor-axis profiles, it appears that most of the features seen in the light profiles represented by the solid lines are real, since they are also observed in the *under*subtracted light profiles. Moreover, a qualitative comparison of both the major and the minor-axis profiles (solid lines) shows that the apparent truncations in or steepening of the major-axis light profiles

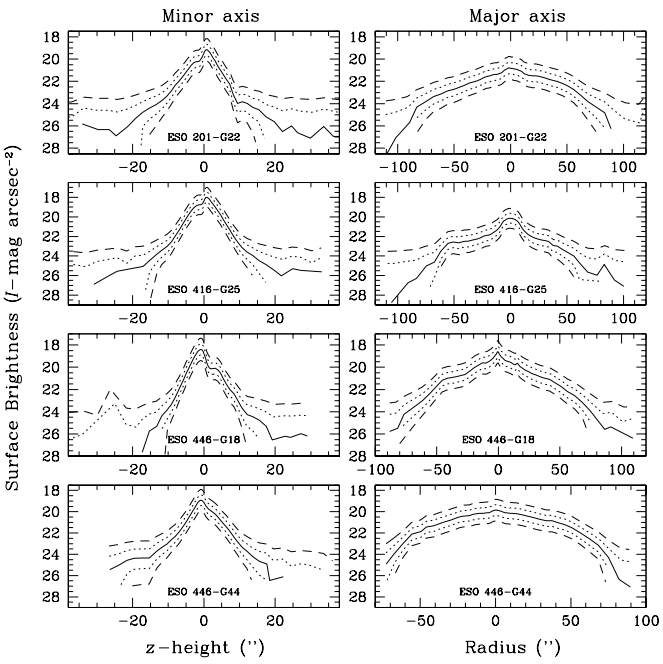

Figure 5. Minor-axis (left-hand panels) and major-axis (right-hand panels) *I*-band luminosity profiles of our sample galaxies. From top to bottom, the lines in each panel represent the minor axis profiles -2σ (dashed), -1σ (dotted), the profiles after subtraction of our best estimates for the sky background, $+1\sigma$ (dotted lines), and $+2\sigma$ (dashed lines), where σ corresponds to the sky noise in the regions that were used to determine the sky background levels. For reasons of clarity, the dashed and dotted profiles are displaced by, respectively, ±1.0 and ±0.5 mag from the solid lines.

do not correspond to similar cut-offs in the minor-axis profiles in any of our sample galaxies. We thus conclude that these features are not due to inaccurate sky subtractions, but represent real deviations from the radial exponential light profiles.

Alternatively, the detection of radially truncated discs can be artificially enhanced if the discs are strongly warped. In fact, it appears that for a number of our sample galaxies the locus of maximum intensity may deviate from the main galactic plane direction (de Grijs 1997). However, this effect is negligible for the determination of their radial truncations, because the deviations are almost insignificant and we average the radial luminosity profiles over a sufficiently large vertical range to avoid such problems.

In addition, effects due to the galaxies' positions near the CCD edge or to scattered light from foreground stars are potentially serious. For the four sample galaxies studied in this paper, the former are non-existent. As one can see in Fig. 1, both ESO 201-G22 and ESO 446-G18 suffer from the superposition of foreground stars, but only in the case of ESO 446-G18 this precludes us from determining its maximum disc radius on the northern end; the superposed foreground star near the eastern edge of ESO 201-G22 is located sufficiently far away from the truncation region, and is found on the most obscured side of the galactic plane.

3.4 Properties of truncated discs

3.4.1 Where do the truncations occur?

In Fig. 6 we show the parallel radial surface brightness profiles (Sect. 2.2.2) of our sample galaxies in all passbands and out to either the edge of the CCD fames or to those radii where the background noise dominates. The dashed lines indicate exponential model discs (Sect. 3.1). From this figure it is immediately clear that the observed surface brightness profiles are significantly fainter in the outer regions than the model discs for all galaxies in our sample and for all passbands in which we have observations.

It is not straightforward, however, to determine the truncation radii of these galactic discs unambiguously. The use of our definition of the truncation radius, $R_{\rm max}$, implies that at $R_{\rm max}$ the surface brightness profiles disappear asymptotically into the background noise. By definition, the S/N ratio at this radius is therefore < 1, and this prevents us from using an automated fitting routine to obtain reliable values for $R_{\rm max}$. In addition, due to the erratic behaviour at large radii of the majority of the profiles in Fig. 6, and the difficulty in the unambiguous determination of the start of teh truncation region, the fitting of Eq. (2) to our observed profiles will not converge to a unique solution.

Therefore, we are forced to estimate the actual disc truncation radii of our sample galaxies by (manually) extrapolating the observed surface brightness profiles to those radii where they would (supposedly) asymptotically disappear into the noise (see the arrows in Fig. 6), as has been done previously by other workers in this field. Thus, the values for the truncation radii listed in Table 4 should be considered *lower limits*; the corresponding uncertainties are our best estimates for the observational errors.

For a comparison with previously published results for other galaxies, we have also included the estimated truncation radii in units of the galaxies' *I*-band scalelengths. We chose to use the *I*-band scalelengths to determine the $R_{\rm max}/h_R$ ratios, because these represent our longest-wavelength observations, which most likely best approximate the dominant stellar luminosity (and presumably mass) distributions (de Grijs et al. 1997, de Grijs 1998). The corresponding errors reflect the uncertainties in the determinations of both the scalelengths and the truncation radii.

The discs of both ESO 201-G22 and ESO 446-G18 are truncated at similar radii as found by KS1–4 and Bottema (1995), expressed in units of their disc scalelengths. Although ESO 416-G25 may, within the uncertainties, have a truncated disc just within KS's r.m.s. scatter, ESO 446-G44 is clearly truncated at much smaller radii. This is the sample galaxy with the greatest scalelength and the only one without a bulge.

3.4.2 Asymmetry and sharpness

In a number of previous studies, it has been shown that the disc truncations do not necessarily occur at the same galactocentric distances or with the same abruptness on either side (e.g., KS1, Jensen & Thuan 1982, Näslund & Jörsäter 1997, Abe et al. 1999, Fry et al. 1999). In most cases, however, the truncation radii on either side of the galactic disc occur within $\sim 10-15\%$ of each other. Close examination of

Table 4. Disc truncations in our sample galaxies
Columns: (1) Galaxy name; (2) Passband observed in; (3) Side of the galactic centre; (4) and (5) Cut-off radius (lower limit) and observational error (arcsec); (6) and (7) Cut-off radius (in units of the I-band scalelength) and observational error; (8) Truncation length (arcsec; typical observational uncertainties are of order $\geq 10''$); (9) and (10) Scalelength in the truncation region and observational error, in arcsec; (11) and (12) Scalelength in the truncation region and observational error, in kpc (based on the heliocentric velocities obtained by Mathewson, Ford & Buchhorn 1992 [see de Grijs 1998])

Galaxy	Band	Side	$R_{\rm max}$	$\pm$	$R_{\rm max}$	$\pm$	δ	$h_{R,\delta}$	$\pm$	$h_{R,\delta}$	$\pm$
(ESO-LV)			($''$)		($h_{R,I}$)		($''$)	($''$)		(h^{-1} kpc)	
(1)	(2)	(3)	(4)	(5)	(6)	(7)	(8)	(9)	(10)	(11)	(12)
201-G22	*B*	E	113	10	4.8	0.5	43	14.2	1.0	3.0	0.2
		W	101	4	4.3	0.3	52	16.8	0.9	3.6	0.2
	V	E	101	3	4.3	0.3	18	16.4	0.3	3.5	0.1
		W	99	10	4.2	0.5	50	15.7	0.4	3.4	0.1
	I	E	109	10	4.7	0.5	28	17.6	0.3	3.8	0.1
		W	89	8	3.8	0.4	31	12.9	0.2	2.8	0.1
416-G25	*B*	N	75	5	3.4	0.4	15	6.2	1.6	1.7	0.4
		S	75	10	3.4	0.5	30	10.6	1.4	2.9	0.4
	V	N	87	10	3.9	0.6	29	7.2	1.0	2.0	0.3
		S	96	15	4.3	0.8	56	14.9	0.3	4.1	0.1
	I	N	90	15	4.1	0.8	38	9.2	1.7	2.6	0.4
		S	78	10	3.5	0.5	55	14.3	1.3	4.0	0.4
446-G18	*B*	S	85	8	4.7	0.6	37	11.6	0.6	2.8	0.1
	V	S	82	8	4.5	0.6	34	10.3	0.3	2.5	0.1
	I	S	86	8	4.8	0.6	38	9.8	1.0	2.4	0.2
446-G44	*B*	E	82	10	2.4	0.3	33	12.1	0.2	1.9	0.1
		W	83	10	2.4	0.3	34	9.1	0.9	1.4	0.1
	V	E	84	10	2.4	0.3	36	10.3	1.6	1.6	0.3
		W	83	10	2.4	0.3	35	9.1	1.0	1.4	0.2
	I	E	85	8	2.4	0.3	38	11.7	0.3	1.8	0.1
		W	83	10	2.4	0.3	35	10.2	0.3	1.6	0.1

the profiles in Fig. 6 and of our estimates for $R_{\rm max}$ in Table 4 shows that in general, the discs of our sample galaxies are truncated at similar radii, within their observational uncertainties, although the disc of ESO 201-G22 may be asymmetric by 10–15% in $R_{\rm max}$. The difference between $R_{\rm max}$ determined on either side of its disc is significantly greater than can be accounted for by our error estimates. However, one should be cautious in interpreting this as a real physical difference, because of (i) the unknown effects of the background noise and (ii) the small differences in photometric depth of our observations for each galaxy, which may not reach out to the same radii in all passbands.

Table 4 also contains our best estimates for the extent of the truncation region, δ, and the sharpness with which the luminosity decreases to below the background noise level, expressed in $h_{R,\delta}$, i.e. a measure of the scalelength in the truncation region. The errors in the truncation scalelengths are observational errors, resulting from the comparison of several similar fits in which we adjusted the inner boundary of the radial fitting range by 10–20% (as outer boundary we used $R_{\rm max}$); the formal errors were in general $\leq 1\%$. The combination of both δ and $h_{R,\delta}$ gives us an indication of the asymmetry and sharpness of the actual disc truncations[§].

Our estimates of δ are complicated by the often significant deviations from the simple functionality of Eq. (2) (thus making it difficult to obtain good estimates for the inner boundaries of the truncation regions) and by the large uncertainties associated with our estimates for $R_{\rm max}$, in particular due to their nature as lower limits.

With the exception of the disc of ESO 416-G25, it appears that our sample galaxies are fairly symmetric, in terms of both the sharpness of their disc truncations and the truncation length. Considering the large systematic and observational errors that cannot be avoided at this point, we cannot claim that we detect any systematic asymmetries. However, the disc of ESO 416-G25 is clearly significantly more asymmetric, which cannot be explained by a combination of systematic and observational errors. The northern edge of its disc is very sharply truncated (i.e., its luminosity decreases into the background noise over a much shorter region and with a significantly smaller scalelength) compared to the southern edge. Upon close examination of the actual CCD images, we believe that this may be explained by the fact that we likely observe the outer stellar envelope of an unusually bright[¶] spiral arm, whereas on the southern side we

[§] Use of the parameter δ by itself does not give us a good indication of the sharpness of the truncation: even an infinitesimally sharply truncated disc will be observed to have a finite truncation region due to projection and line-of-sight integration effects. However, the combination of both δ and $h_{R,\delta}$ constrains our discussion about the disc asymmetries more strongly than the use of $h_{R,\delta}$ alone.

[¶] The surface brightness at these radii is clearly in excess of the

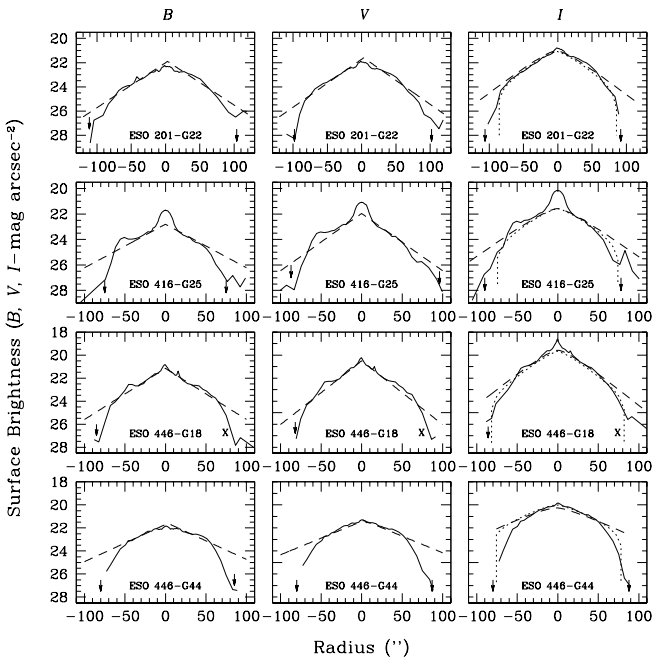

Figure 6. Radial surface brightness profiles of our sample galaxies taken along their major axes. Overplotted are the model exponential profiles (dashed lines), based on our 2D surface brightness modelling. The arrows indicate the measured truncation radii; for ESO 446-G18 the crosses indicate the side where we cannot determine the maximum radius due to the presence of foreground stars. The observational uncertainties are dominated by the noise in the profiles. The dotted lines in the *I*-band panels correspond to our 2D sharply truncated models, as described in Sect. 3.4.2.

are looking into the inside of a spiral arm. Note, however, that also at the southern edge of the disc a clear truncation signature is observed (Fig. 6).

The last two columns of Table 4 show that in none of our sample galaxies the radial scalelength in the truncation region decreases to values of order or less than 1 kpc, as was found previously by a number of studies (see Sect. 1). Using $H_0 \sim 50$ km s^{-1} Mpc^{-1}, or other values closer to the current best estimate, will further increase the truncation scalelengths measured in our galaxies. We are therefore forced to conclude that, although our discs are clearly truncated, the truncation occurs over a larger region and not as abruptly as found by, e.g., KS1–4 for a number of the largest edge-on galaxies in the northern hemisphere.

In the *I*-band panels of Fig. 6, we also show the corresponding profiles of a symmetric, projected, sharply truncated exponential disc, with the disc truncations occurring at $R_{\rm max}$ (dotted lines). These profiles were obtained by applying the method used to extract the observed profiles used for Fig. 6 to 2D model images of our sample galaxies, for which the scale parameters from the 2D surface brightness modelling were used. From a comparison between these dotted lines and the actual, observed profiles, it is clear that the discs of our sample galaxies are generally not infinitesimally sharply truncated, but show a more gradual decrease of their radial luminosity density, perhaps with the exception of ESO 446-G18. These figures also show qualitatively that any asymmetries between both sides of the galactic discs are small; for an initial qualitative comparison, the sharply truncated model profiles are very helpful in guiding the eye to detect asymmetries.

Finally, from an inspection of the values for the ratio of $R_{\rm max}/h_R$ (Table 4), no apparent trend with wavelength can be discerned, within the observational errors. However, a detailed comparison of the radial $(B-I)$ colour profiles, our longest colour baseline, reveals that the disc colour tends to get bluer in the truncation region compared to the colours in the main disc. A similar result was obtained by Sasaki (1987) for the truncation region of NGC 5907. Although this may be indicative of more recent star formation at the edge of the discs (see Sect. 4.2), the opposite behaviour is exhibited on the northern side of the disc of ESO 416-G25, where the disc colour becomes dramatically redder in the truncation region. This is confirmed by the fact that its disc appears to be more sharply truncated in the *B* band compared to the *I*-band observations. As mentioned above, this behaviour may be explained if – at that side of the galactic disc – we are observing the outside stellar envelope of a spiral arm, which thus causes a sharply truncated stellar distribution.

4 GALACTIC DISCS

4.1 The formation of exponential discs

Although it has been established observationally that the stellar discs of both high surface brightness spiral galaxies (e.g., de Jong 1995) and of non-dwarf low surface brightness galaxies (e.g., Dalcanton, Spergel & Summers 1997, and references therein) display a largely exponential behaviour, the physical explanation for this simple form of the radial luminosity density distribution is still controversial. The major difficulty in explaining this for all these galaxy types is that any model that attempts to do so must also explain *both* the large range of surface brightnesses and scale parameters among galactic discs *and* the similarities among disc galaxies, such as the asymptotically flat rotation curves observed in most disc galaxies (e.g., Bosma 1981, Begeman, Broeils & Sanders 1991, Persic & Salucci 1995, de Blok, McGaugh & van der Hulst 1996, Swaters 1999 and references therein) and the universal nature of the Tully-Fisher (1977) relation (e.g., Strauss & Willick 1995, Zwaan et al. 1995, Sprayberry et al. 1995). Such similarities imply that the basic formation mechanism for all disc galaxies is similar and may depend on the primordial properties of their protogalaxies (e.g., Dalcanton et al. 1997).

In general, models that attempt to explain the exponential nature of galactic discs can be divided into two categories, namely those that create an initial exponential gas disc, in which subsequent star formation takes place (e.g., Mestel 1963, Freeman 1970, Larson 1976, Fall & Efstathiou 1980, Gunn 1982, Seiden et al. 1984, van der Kruit 1987, Dalcanton 1997) and those in which the gas in the disc is radially redistributed by viscous torques to form an exponential distribution (e.g., Silk & Norman 1981, Lin & Pringle 1987, Clarke 1989, Yoshii & Sommer-Larsen 1989).

expected contribution of the exponential model disc; adjusting the scale length of the model disc cannot resolve this problem.

4.1.1 Disc formation through (proto-)halo collapse

Mestel (1963) noticed that the specific angular momentum distribution of the Galactic disc, as well as those of the discs of a few other galaxies (Crampin & Hoyle 1964) and of *self-gravitating* exponential discs, approximate that of a uniformly rotating, uniform sphere, for which applies that (Mestel 1963)

$$M(h_\mathrm{s})/M = 1 - (1 - h_\mathrm{s}/h_\mathrm{max})^{3/2} \quad (7)$$

where $M(h_\mathrm{s})/M$ is the fraction of the mass that has specific angular momentum $\leq h_\mathrm{s}$. Van der Kruit (1988) has shown that this distribution approximates the exponential disc very well for the particular case that the maximum specific angular momentum of the disc $h_\mathrm{max} \simeq 4.5 h_R V_\mathrm{max}$, where V_max is the maximum rotational velocity.

The deviation from an infinite exponential disc becomes larger as $M(h_\mathrm{s})/M$ approaches unity, because the uniform sphere has a maximum specific angular momentum, whereas the infinite exponential disc does not. Therefore, if disc material starts out with distribution (7) and settles in a disc via detailed conservation of angular momentum in a force field corresponding to a flat rotation curve we may expect the result to be a roughly exponential disc (Gunn 1982) with a truncation at about $4.5 h_R$ (van der Kruit 1987), even with a modest degree of radial angular momentum redistribution and continuous infall of extragalactic gas clouds (e.g., Lacey & Fall 1985).

However, Dalcanton et al. (1997) point out that because of the assumption of a flat rotation curve, the constraints for the final disc/halo combination to be in gravitational equilibrium are not always met in such model scenarios. Therefore, they (Dalcanton et al. 1997) expanded upon the earlier disc formation scenarios by allowing for a responsive (i.e., non-static) dark-matter halo, while retaining the assumption that the collapse time is much shorter than the angular momentum redistribution time. They then also conclude that roughly exponential discs that obey the Tully-Fisher relation are formed from the collapse of a uniform gas cloud that has experienced a uniform external torque.

4.1.2 Disc formation through viscous processes

Alternatively, Yoshii & Sommer-Larsen (1989) show that the fundamental condition for producing the exponential stellar distribution is that the star formation time scale is comparable to the time scale for viscous evolution of the disc. When this condition is met in a differentially rotating disc, the final stellar distribution becomes exponential largely irrespective of the specific form of the initial gas distribution or the specific process of viscosity (Lin & Pringle 1987). Yoshii & Sommer-Larsen (1989) argue that there are two plausible physical star forming processes that can result in comparable time scales for both the star formation and the viscous disc evolution. These are the gravitational instability of the disc structure itself and the collisions among interstellar clouds; both processes give rise to kinetic viscosities:

- If a gravitational instability arises, the gaseous disc will be kept on the verge of instability, since the cooling of the gas will be counteracted by the heating caused by the instability. As a consequence of this instability, stars will form in the disc with a time scale comparable to that of the viscous evolution.
- The role of inelastic intercloud collisions is that the kinetic energy is dissipated through radiation and that the increase of random motions is counteracted by this process. Thus, since the star formation is also induced in the overdense region in colliding clouds, the viscous time scale, which is related to the collision time scale of clouds, is probably comparable to the star formation time scale.

Simultaneously, Clarke (1989) arrived at the same conclusion, but found that she needed to impose an outer cut-off on the star forming disc to be able to reproduce the radial distribution of stars, gas and metallicities observed in a wide range of galaxy types for various viscosity and star formation laws. More specifically, she found that realistic exponential discs are formed by a combination of viscous evolution and star formation, independent of the initial mass profile, and the detailed rotation, viscous and star formation laws, if an outer disc cut-off is present. The ratio of viscous to dynamical time scale at the star formation edge needs to be only of order 100.

4.2 The origin of truncated discs

Although many disc-dominated galaxies, including the Galaxy, feature relatively sharp truncations in their radial light distributions at the outer edges of their discs, this does not necessarily imply a similarly steep decline in the disc mass distribution. In Sect. 1.2 we argued that the Galactic stellar mass distribution shows evidence for an abrupt cut-off at a few kpc from the Sun, which was based on detailed observations of various mass-tracing disc components.

The situation for other galaxies is less clear, however. Based on detailed observations of the warping edge-on galaxy NGC 4013, Bottema (1995) argues that the fact that the HI warp abruptly starts at the truncation radius implies that the cut-off in the light distribution corresponds to a similar truncation in the disc mass distribution. If correct, then an external gravitational disturbance can easily generate the warping of the HI layer. This hypothesis is supported by observations of other warped galaxies, which show a similar behaviour (e.g., Sancisi 1983, Sancisi & van Albada 1987). For a few galaxies for which detailed rotation curves are available, such as NGC 891, NGC 4013, and NGC 5907, the truncation radius corresponds to a sudden decrease of the rotation velocity, implying a similar decrease in the disc mass density (Casertano 1982, Bahcall 1983, Bottema 1995, 1996; see Sect. 4.3).

The origin of the cut-offs and their asymmetry and sharpness pose interesting constraints on theories of galaxy formation; its presence suggests that there is no feedback process that strongly controls the disc stability (e.g., Elmegreen & Parravano 1994).

A number of formation scenarios for sharp disc cut-offs have been proposed, which are not necessarily mutually exclusive.

4.2.1 Subcritical gas densities

It is often assumed that star formation has ceased at the truncation radius due to the lower-than-critical HI density beyond the radius where the gas is allowed to be stable (e.g., Quirck 1972, Fall & Efstathiou 1980, KS1, Gunn 1982, Lacey & Fall 1985, Athanassoula & Bosma 1988, Kennicutt 1989, Bosma & Freeman 1993, Wang & Silk 1994), which corresponds to an upper limit for the HI mass density of about 1.5 orders of magnitude below that presently observed in the solar neighbourhood (KS3). In fact, the observation that the HI gas distribution in galactic discs is often much more extended than the stellar or molecular gas discs implies that some kind of star formation threshold should be present. Fall & Efstathiou (1980) suggested that the truncations in disc galaxies occur at those radii at which the shear due to differential rotation is more effective than the self-gravity in the primordial disc, so that star formation is hindered. This is, in fact, the condition for stability derived by Toomre (1964) and Goldreich & Lynden-Bell (1965).

Kennicutt (1989) showed convincingly, based on detailed observations of the star formation in a sample of spiral galaxies, that gravitational stability regulates both the star formation rate and the gas distributions in galactic discs (following Quirck 1972). This is equivalent with the assumption that if gas in disc galaxies is unstable, efficient star formation will deplete the gas until it is just barely stable at or just below the critical density for star formation, thus leading to values of Toomre's (1964) Q parameter for stability of galactic discs close to unity (e.g., Kennicutt 1989, Wang & Silk 1994). This scenario naturally leads to a cut-off in the star formation rate. If the abrupt decrease in the star formation rate at the threshold radius persists sufficiently long, a visible truncation in the stellar radial luminosity profiles is expected to arise (Kennicutt 1989). However, the Toomre (1964) and Goldreich & Lynden-Bell (1965) stability criterion appears to be a poor predictor for $R_{\max}$ (KS3).

A slightly different mechanism was proposed by Elmegreen & Parravano (1994). They hypothesise that star formation stops at the optical edge of a galaxy because the pressure is too low for the occurrence of turbulence or shock waves to drive the gas into a low-temperature bound phase (see also Braine, Brouillet & Baudry 1997), thus preventing continuing star formation. This scenario also explains naturally why the HI gas is often distributed in much more extended disc structures than the stellar component (Braine et al. 1997).

4.2.2 Slow disc formation

Alternatively, in a scenario with slow disc formation (e.g., Larson 1976), the truncation radius might be the radius where the disc formation time equals the present age of the galaxy. Such models, which include the so-called stochastic self-propagating star formation scenario (SSPSF) of Seiden (1983) and Seiden et al. (1984), predict a long time scale for the formation of the outer part of the disc, implying a significant gas content and SFR in the disc even after 10^{10} yr. Larson (1976) argues that in the outer parts of the disc the time scale for disc growth is dominated by the long time scale required for star formation at the corresponding low gas densities. Therefore, this model does not exclude the star formation threshold scenario discussed in the previous section. An additional spin-off of the SSPSF theory is that discs are formed with a radial luminosity dependence $\propto 1/R$ minus a constant; this functional form resembles an exponential distribution over a wide range of galactic radii, and the extrapolated disc central surface brightnesses for (model) galaxies with different absolute densities but similar HI content are all the same (cf. Freeman 1970).

Gunn (1982) suggested that galactic discs are formed relatively slowly from infalling material, so that in the outer parts the disc formation has not yet ceased. In fact, many spiral galaxies have HI gas beyond the truncation edge, which could be material that they collected at a later stage from their surroundings, after the inner disc out to $R_{\max}$ formed quickly. Van der Kruit (1987, 1988) argues that this is not unreasonable in view of the fact that this HI often is in warped layers.

Sasaki (1987) pointed out that, assuming that the disc stars are the same as those of open clusters, the mean age of stars decreases with increasing distance from the centre, as indicated by, e.g., the increasingly blue appearance of the disc of NGC 5907 with radius. The sharp cut-off at the edge of the disc of this galaxy is expected to be washed out in 2×10^9 years due to random motion. Since the mean age indicated by the colour at the outermost part of the disc is shorter than this washing-out time, the smearing-out procedure of the sharp cut-off may be considered to be still under way. Similarly, all of our four sample galaxies studied in this paper show significant radial colour gradients, corresponding to bluer disc colours at larger radii, even at those radii where the effects of in-plane extinction are negligible (de Grijs 1997 [Chapter 9]), lending support for this slow disc formation scenario.

As we argued in Sect. 3.4, the occurrence of a density threshold for star formation, combined with a slowly growing galactic disc, can be tested directly by a multi-colour study of both the galactocentric distances at which the discs truncate, and a comparison of their sharpness as a function of wavelength. Since the bluest optical disc colours correspond to the youngest population of disc stars, a slowly growing disc will exhibit cut-offs at larger galactocentric distances in the bluer passbands compared to those seen at redder wavelengths. This scenario will also result in shallower cut-offs in the redder passbands than in the bluer observations, due to standard stellar and galactic disc evolution. This may be what we observe in ESO 416-G25, as is evidenced by the redder colours in the truncation region on the northern side compared to the main disc colours (Sect. 3.4.2), although we cannot confirm this scenario for any of the other galaxies in our sample.

4.2.3 Tidally induced disc truncations

Finally, tidal interactions between neighbouring galaxies may be the cause of sharp disc truncations in individual cases (e.g., Jensen & Thuan 1982, Sasaki 1987, Bottema 1995), as shown in numerical simulations by, e.g., Noguchi & Ishibashi (1986). These authors show that tidal features, including an outer ring structure formed in the later stages, can arise due to close encounter of two spiral galaxies. Such a ring structure can mimic the presence of a truncated ex-

ponential disc (see also Bosma & Freeman 1993). It is, however, unlikely that tidal effects are the origin of all radially truncated galactic discs (e.g., Sasaki 1987), although most galaxies previously thought to be isolated, e.g., NGC 5907 (Sancisi 1976; Cox et al. 1996) do have nearby neighbours, although not necessarily close (e.g., Sasaki 1987). For none of our sample galaxies neighbours at similar redshifts have been detected at *projected* distances closer than $\sim 10.'4$ (ESO 416-G25; $10.'4 \simeq 0.35$ Mpc for $H_0 = 50$ km s^{-1} Mpc^{-1}); in fact, except for ESO 416-G25, they are all classified as field galaxies (Lauberts 1982). It is therefore unlikely that the disc truncations in our sample galaxies are due to tidal interactions in all cases.

4.3 Dynamical consequences of disc truncations

4.3.1 Edge smearing constraints and disc asymmetries

The persistence of the sharp cut-offs found by, e.g., KS1–4 places a strong upper limit on the stellar velocity dispersion at the disc edge (KS1). Adopting a rotational velocity of 250 km s^{-1} at 20 kpc for NGC 4565, the radial stellar velocity dispersion, $\langle v_R^2 \rangle^{1/2}$, must be ≤ 10 km s^{-1} so that random motions do not wash out the sharp cut-off within one revolution time (Jensen & Thuan 1982; see also KS1, May & James 1984), or the sharp cut-off must be a transient feature (e.g., Sasaki 1987). This low upper limit for $\langle v_R^2 \rangle^{1/2}$ is close to the minimum value of ~ 2 km s^{-1} needed to satisfy Toomre's (1964) criterion of local stability for disc galaxies, and thus for star forming activity.

Alternatively, in the case of a disc formation scenario in which the disc grows outward (Sect. 4.2.2) a sharp edge can be maintained if this outward growth is sufficiently rapid, so that the random motion of the stars does not smear out the edge. Note, however, that the disc truncations in our sample galaxies are not as sharp as those found by KS1–4, among others, which will relax these requirements.

The situation becomes more complicated if the galactic disc is lopsided or if the truncations occur at different radii. Following the epicyclic description of Baldwin, Lynden-Bell & Sancisi (1980), van der Kruit (1988) estimates a smearing time of 1.7×10^{10} yr for the Galactic disc, and he concludes that a variation in the truncation radii of order 10% may just survive a Hubble time. With the exception of ESO 416-G25, our sample galaxies appear to comfortably meet this requirement.

4.3.2 Rotation curves as diagnostic tools

Casertano (1983) has shown that a truncated stellar disc leaves a signature on the rotation curve in the form of a region of slowly varying velocity followed by a steep decline in velocity just outside the truncation radius (see also Hunter, Ball & Gottesman 1984). The amount of this decrease is a measure of the disc mass.

The effect of a truncation is a *flattening* of the rotation curve inside the truncation itself, from some radius R_0 to $R_{\rm max}$, and a steeper decrease of the velocity outside. For some values of the cut-off radius, including that of NGC 5907, the rotation curve appears to be flat (within 5%) between $R \simeq 2h_R$ and $R \simeq R_{\rm max}$ (Casertano 1983).

The well-known warped edge-on galaxy NGC 4013, for which Bottema (1995) suspected a sudden decrease in the mass density corresponding to the truncation radius, has indeed been shown to exhibit a sudden drop in the rotational velocity of about 20 km s^{-1} just at the optical edge (Bottema, Shostak & van der Kruit 1987, Bottema 1995, 1996). This drop can be understood if one realises that near the edge of the galactic disc the mass distribution will be irregular: there is no smooth, circular end to the disc, but it likely ends in spiral arms. Bottema (1996) argues that therefore gas moving in the potential of such patches of stellar matter will not be in precise circular motion and hence the radial velocity along the line of sight is somewhat lower than the true rotation.

Finally, Bahcall (1983) showed that, for Sb or Sc galaxies like NGC 891 or the Galaxy, the feature in the rotation curve due to the truncated stellar disc is observable only if the truncation radius $\leq 4h_R$ (smaller for galaxies with more prominent bulges), if the region where the cut-off occurs is small compared to h_R, and if the halo mass inside the truncation radius is smaller than the disc mass (Casertano 1983).

Unfortunately, the currently available velocity information for the four galaxies in our pilot sample (in fact, for the entire de Grijs [1998] sample), does not allow us to confirm the presence of sharp truncations in the disc mass based on the shape of the rotation curves: only for ESO 446-G18 and ESO 446-G44 rotation curves have been published, for the Hα emission (Mathewson et al. 1992) and the HI component (Persic & Salucci 1995, based on the raw Mathewson et al. 1992 data), but these rotation curves do not or just barely reach those galactocentric distances where we expect to be able to see a truncation signature. The availability of reliable rotation curves extending all the way to the discs' edges would therefore be a great asset for a follow-up study of disc truncations.

5 SUMMARY AND CONCLUSIONS

In this paper we have presented the first results of a systematic analysis of radially truncated exponential discs for a pilot sample of four disc-dominated edge-on spiral galaxies with particularly noticeable cut-offs. Edge-on galaxies are very useful for the study of truncated galactic discs, since we can follow their light distributions out to larger radii than in less highly inclined galaxies.

We have shown that these features are not caused by inaccurate sky subtraction, but are real deviations from the radial exponential light profiles. In view of the finite extent of the cut-off region and to avoid discontinuities in the luminosity and density distributions, we have adopted Casertano's (1983) "soft cut-off" of the radial density distribution in the truncation region. This assumes that in the truncation region the radial luminosity density decreases linearly to zero.

An independent approach to obtain the statistics of truncated galactic discs, using a sample of galaxies selected in a uniform way, is needed in order to better understand the overall properties and physical implications of this feature. The origin of these truncations and their asymmetry and sharpness are helpful to better constrain theories of galaxy

formation; if the truncations seen in the stellar light are also present in the mass distribution, they would have important dynamical consequences at the disc's outer edges. In fact, we have shown that the truncated luminosity distributions of our pilot sample galaxies, if also present in the mass distributions appear to comfortably meet the requirements for longevity.

The truncation radii, expressed in units of $R_{\max}/h_R$, for the discs of both ESO 201-G22 and ESO 446-G18 are similar to those found by KS1–4 and Bottema (1995). Although ESO 416-G25 may, within the uncertainties, have a cut-off radius just within KS's r.m.s. scatter, ESO 446-G44 is clearly truncated at much smaller radii. In general, the discs of our sample galaxies are truncated at similar radii on either side of their centres, within the observational uncertainties, although the disc of ESO 201-G22 may be asymmetric by 10–15%.

With the exception of the disc of ESO 416-G25, it appears that our sample galaxies are fairly symmetric, in terms of both the sharpness of their disc truncations and the truncation length, although the truncations occur over a larger region and not as abruptly as found by, e.g., KS1–4. The northern edge of the disc of ESO 416-G25 is very sharply truncated compared to the southern edge. We believe that this may be explained by the fact that we likely observe the outer stellar envelope of an unusually bright spiral arm, whereas on the southern side we are looking into the inside of a spiral arm.

Stability requirements for galactic discs may play an important role in the formation of disc truncations. At the outer disc edges, efficient star formation will deplete the gas until it is just barely stable (e.g., Kennicutt 1989), thus leading to a cut-off in the star formation rate. If the abrupt decrease in the star formation rate at the threshold radius persists sufficiently long, a visible truncation in the stellar radial luminosity profiles is expected to arise. Such a scenario, in which galactic discs are truncated at the radii where the gas density becomes subcritical for star formation to occur, combined with slowly growing discs (e.g., Larson 1976), may well be just what we observe in our sample galaxies. This hypothesis is supported by the detailed comparison of the radial $(B-I)$ colour profiles (Sect. 3.4.2), showing that the disc colour tends to get bluer, on average, in the truncation region compared to the colours in the exponential disc. Such colour distributions are generally seen in spiral discs, and are often interpreted in terms of increasingly younger ages with increasing galactocentric distance.

Acknowledgments

We thank Piet van der Kruit for stimulating discussions. This work is partially based on the undergraduate senior thesis of KHW at the University of Virginia. RdeG acknowledges funding from NASA grants NAG 5-3428 and NAG 5-6403 and hospitality at the Kapteyn Institute of the University of Groningen. This research has made use of NASA's Astrophysics Data System Abstract Service and of the NASA/IPAC Extragalactic Database (NED) which is operated by the Jet Propulsion Laboratory, California Institute of Technology, under contract with the National Aeronautics and Space Administration.

REFERENCES

Abe F., Bond I.A., Carter B.S., et al., 1999, AJ, 118, 261
Andredakis Y.C., Sanders R.H., 1994, MNRAS, 267, 283
Athanassoula E., Bosma A., 1988, in: Large Scale Structures in the Universe, IAU Symposium 130, eds. Audouze J., Pelletan M.-C., Szalay A., Dordrecht: Reidel, p. 391
Bahcall J.N., 1983, ApJ, 267, 52
Baldwin J.E., Lynden-Bell D., Sancisi R., 1980, MNRAS, 193, 313
Barnaby D., Thronson Jr. H.A., 1992, AJ, 103, 41
Barteldrees A., Dettmar R.-J., 1994, A&AS, 103, 475
Barton I.J., Thompson L.A., 1997, AJ, 114, 655
Begeman K., Broeils A.H., Sanders R.H., 1991, MNRAS, 249, 523
Bosma A., 1981, AJ, 86, 1791
Bosma A., Freeman K.C., 1993, AJ, 106, 1394
Bottema R., 1995, A&A, 295, 605
Bottema R., 1996, A&A, 306, 345
Bottema R., Shostak G.S., van der Kruit P.C., 1987, Nat, 328, 401
Braine J., Brouillet N., Baudry A., 1997, A&A, 318, 19
Burton W.B., 1988, in: Galactic and Extragalactic Radio Astronomy, eds. Verschuur G.L., Kellerman K.I., New York: Springer, p. 295
Casertano S., 1983, MNRAS, 203, 735
Chromey F.R., 1978, AJ, 83, 162
Clarke C.J., 1989, MNRAS, 238, 283
Cox A.L., Sparke L.S., van Moorsel G., Shaw M., 1996, AJ, 111, 1505
Crampin D.J., Hoyle F., 1964, ApJ, 140, 99
Dalcanton J.J., Spergel D.N., Summers F.J., 1997, ApJ, 482, 659
de Blok, W.J.G., McGaugh S.S., van der Hulst J.M., 1996, MNRAS, 283, 18
de Grijs R., 1997, PhD Thesis, Univ. of Groningen, the Netherlands
de Grijs R., 1998, MNRAS, 299, 595
de Grijs R., Peletier R.F., 1997, A&A, 320, L21
de Grijs R., Peletier R.F., van der Kruit P.C., 1997, A&A, 327, 966
de Grijs R., van der Kruit P.C., 1996, A&AS, 117, 19
de Jong R.S., 1995, PhD Thesis, Univ. of Groningen, the Netherlands
de Vaucouleurs G., 1948, Ann. Astrophys., 11, 247
de Vaucouleurs G., Capaccioli M., 1979, ApJS, 40, 699
Duval M.F., Athanassoula E., 1983, A&A, 123, 297
Elmegreen B.G., Parravano A., 1994, ApJ, 435, L121
Fall S.M., Efstathiou G., 1980, MNRAS, 193, 189
Fich M., Blitz L., 1984, ApJ, 279, 12
Fich M., Blitz L., Stark A.A., 1989, ApJ, 342, 272
Freeman K.C., 1970, ApJ, 160, 811
Freudenreich H.T., 1998, ApJ, 492, 495
Freudenreich H.T., Berriman G.B., Dwek E., et al., 1994, ApJ, 429, L69
Fry A.M., Morrison H.L., Harding P., Boroson T.A., 1999, AJ 118, 1209
Giovanelli R., Haynes M.P., Salzer J.J., Wegner G., Da Costa L.N., Freudling W., 1994, AJ, 107, 2036
Goldreich P., Lynden-Bell D., 1965, MNRAS, 130, 97
Gunn J.E., 1982, in: Astrophysical cosmology, Proceedings of the Study Week on Cosmology and Fundamental Physics, Vatican City State, p. 233
Henderson A.P., Jackson P.D., Kerr F.J., 1982, ApJ, 263, 116
Hunter Jr. J.H., Ball R., Gottesman S.T., 1984, MNRAS, 208, 1
Jensen E.B., Thuan T.X., 1982, ApJS, 50, 421
Kennicutt Jr. R.C., 1989, ApJ, 344, 685
Kent S.M., Dame T.M., Fazio G., 1991, ApJ, 378, 131
Knapen J.H., van der Kruit P.C., 1991, A&A, 248, 57

Kregel M., van der Kruit P.C., de Grijs R., 2000, in prep.
Kulkarni S.R., Blitz L., Heiles C., 1982, ApJ, 259, L63
Kylafis N.D., Bahcall J.N., 1987, ApJ, 317, 637
Lacey C.G., Fall S.M., 1985, ApJ, 290, 154
Larson R.B., 1976, MNRAS, 176, 31
Lauberts A., 1982, The ESO/Uppsala Survey of the ESO(B) Atlas, Garching bei München: ESO
Lauberts A., Valentijn E.A., 1989, The Surface Photometry Catalogue of the ESO-Uppsala Galaxies, Garching bei München: ESO (ESO-LV)
Lequeux J., Dantel-Fort M., Fort B., 1995, A&A, 296, L13
Lin D.N.C., Pringle J.E., 1987, ApJ, 320, L87
Marquardt D., 1963, J. Soc. Ind. Appl. Math., 11, 431
Mathewson D.S., Ford V.L., Buchhorn M., 1992, ApJS, 81, 413
May A., James R.A., 1984, MNRAS, 206, 691
Mestel L., 1963, MNRAS, 126, 553
Morrison H.L., Boroson T.A., Harding P., 1994, AJ, 108, 1191
Näslund M., Jörsäter S., 1997, A&A, 325, 915
Noguchi M., Ishibashi S., 1986, MNRAS, 219, 305
Persic M., Salucci P., 1995, ApJS, 99, 501
Porcel C., Battaner E., Jiménez-Vicente J., 1997, A&A, 322, 103
Quirck W.J., 1972, ApJ, 176, L9
Robin A.C., Crézé M., Mohan V., 1992a, A&A, 265, 32
Robin A.C., Crézé M., Mohan V., 1992b, ApJ, 400, L25
Robin A.C., Crézé M., Mohan V., 1996, in: Unsolved Problems of the Milky Way, IAU Symposium 169, eds. Blitz L., Teuben P., Dordrecht: Kluwer, p. 681
Romanishin W.E., Strom K.M., Strom S.E., ApJS, 53, 105
Ruphy S., Robin A.C., Epchtein N., Copet E., Bertin E., Fouqué P., Guglielmo F., 1996, A&A, 313, L21
Sancisi R., 1983, in: Internal Kinematics and Dynamics of Galaxies, IAU Symposium 100, ed. Athanassoula, E., Dordrecht: Reidel, p. 55
Sancisi R., van Albada T.S., 1987, in: Dark Matter in the Universe, IAU Symposium 117, eds. Kormendy J., Knapp G.R., Dordrecht: Reidel, p. 67
Sasaki T., 1987, PASJ, 39, 849
Seiden P.E., 1983, ApJ, 266, 555
Seiden P.E., Schulman L.S., Elmegreen B.G., 1984, ApJ, 282, 95
Shaw M.A., Gilmore G., 1989, MNRAS, 237, 903
Shaw M.A., Gilmore G., 1990, MNRAS, 242, 59
Silk J., Norman C., 1981, ApJ, 247, 59
Sprayberry D., Bernstein G.M., Impey C.D., Bothun G.D., 1995, ApJ, 438, 72
Strauss M.A., Willick J.A., 1995, Phys. Rep., 261, 271
Swaters R.A., 1999, PhD Thesis (Chapter 4), Univ. of Groningen, the Netherlands
Toomre A., 1964, ApJ, 139, 1217
Tully R.B., Fisher J.R., 1977, A&A, 54, 661
van der Kruit P.C., 1987, A&A, 173, 59
van der Kruit P.C., 1988, A&A, 192, 117
van der Kruit P.C., 1989, in: The Milky Way as a Galaxy, eds. Gilmore G., King I., van der Kruit P.C., Geneva: SAAS-FEE, p. 77
van der Kruit P.C., de Grijs R., 1999, A&A, 352, 129
van der Kruit P.C., Searle L., 1981a, A&A, 95, 105 (KS1)
van der Kruit P.C., Searle L., 1981b, A&A, 95, 116 (KS2)
van der Kruit P.C., Searle L., 1981a, A&A, 110, 61 (KS3)
van der Kruit P.C., Searle L., 1981b, A&A, 110, 79 (KS4)
van Dokkum P.G., Peletier R.F., de Grijs R., Balcells M., 1994, A&A, 286, 415
Wang B., Silk J., 1994, ApJ, 427, 759
Wevers B.M.H.R., 1984, PhD Thesis, Univ. of Groningen, the Netherlands
Wouterloot J.G.A., Brand J., Burton W.B., Kwee K.K., 1990, A&A, 230, 21
Xilouris E.M., Kylafis N.D., Papamastorakis J., Paleologou E.V., Haerendel G., 1997, A&A, 325, 135
Yoshii Y., Sommer-Larsen J., 1989, MNRAS, 236, 779
Zwaan M.A., van der Hulst J.M., de Blok W.J.G., McGaugh S.S., 1995, MNRAS, 273, L35